Proceedings of ASME Turbo Expo 2011
GT2011
June 6-10, 2011, Vancouver, British Columbia, Canada

GT2011-45312

DNS OF STAGNATION POINT HEAT TRANSFER AFFECTED BY VARYING WAKE-INDUCED TURBULENCE

Lars Venema*
Dominic von Terzi
Hans-Jörg Bauer

Institut für Thermische Strömungsmaschinen
Karlsruhe Institute of Technology
Kaiserstraße 12, 76131, Karlsruhe
Germany
Email: lars.venema@kit.edu

Wolfgang Rodi

Institut für Hydromechanik
Karlsruhe Institute of Technology
Kaiserstraße 12, 76131, Karlsruhe
Germany

ABSTRACT

In the present study a tandem cylinder setup is simulated by means of embedded DNS. The influence of wake turbulence on the heat transfer in the stagnation region of the rear cylinder is investigated. The oncoming flow is varied by increasing the distance between the two cylinders, causing a change of the turbulent wake characteristics and the heat transfer. The data of both simulations show good agreement with an existing experimental correlation in the literature. For the small wake generator distance, a clear shift of the maximum heat transfer is observed away from the stagnation line. This shift is less pronounced for the larger distance.

NOMENCLATURE

a_1	Free-stream strain-rate
K	Turbulent kinetic energy
l	Wake generator distance
Nu	Nusselt number
Nu_a	Characteristic Nusselt number
Pr	Prandtl number
Re	Reynolds number
T	Temperature
T_0	Free-stream temperature
T_w	Wall temperature
Tu	Turbulence intensity
Tu_a	Characteristic turbulence intensity
u,v,w	Velocities in x,y and z direction
u',v',w'	Velocity fluctuations in x,y and z direction
U_∞	Free-stream velocity
x,y,z	Cartesian coordinates
r,θ,z	Cylindrical coordinates
$\langle\cdot\rangle$	Time-average of $\cdot$

INTRODUCTION

In modern gas turbines, the first turbine stages after the combustion chamber are exposed to hot gases with temperatures well beyond material limits. It is therefore of key importance to understand the physical mechanisms that influence the potentially destructive heat transfer. In the first turbine stages, the boundary layer is largely laminar due to the strong acceleration, but it is subjected to turbulent wakes of the preceding blades. This is a challenging research topic, which has been investigated in a controlled way in the past by replacing the turbine blades with cylinders.

A semi-analytical relation was obtained in [1] for circular cylinders, describing the heat transfer for laminar flow, without any turbulence effects. However, many investigations have

*Corresponding author.

shown that free-stream turbulence causes a considerable increase in heat transfer in the stagnation region and a correlation for this was proposed in [2]. The important parameters in this correlation are, besides the Reynolds number, the turbulence intensity and the free-stream strain rate. The correlation shows two regimes for the heat transfer, one regime is characterized by low turbulence intensity, low Reynolds numbers and high free-stream strain-rates in which a high dependency of the heat transfer on the flow characteristics is seen. The second regime, at high turbulence intensity and Reynolds numbers, shows a less pronounced influence of changes in the oncoming flow. Both correlations are valid for incompressible flow, with small Mach numbers, M.

In [3] experiments were carried out, in which turbulence in a wake generated by an upstream smaller cylinder impinges on a heated cylinder. In the experimental setup, the wake generator distance is relatively small. The oncoming flow is therefore characterized by a high turbulence intensity and a strong wake deficit of the streamwise velocity. Therefore, these experiments cover the second regime in the correlation of [2]. The increase in heat transfer is well documented in this work, but the mechanisms causing it are not well understood. Here a study by Direct Numerical Simulation (DNS) would help to clarify these mechanisms as the results allow to extract all details of the flow development, the turbulent structures and also the heat flux caused by the turbulence.

First DNS inspired by the experiments of [3] were carried out in [4, 5]. These simulations show good agreement with the correlation mentioned above, however, [4] covers mainly the lower regime of the correlation due to a lower Reynolds number and a higher free-stream strain-rate than the experiments. The first simulation to reach the second regime was performed in [5], where the experimental setup of [3] was realized and simulated by means of embedded DNS. The Reynolds number, though, was still lower than in the experiments. Good agreement with the correlation of [2] was found and by flow visualizations it was conjectured that the same physical mechanism was at play as proposed in [4]. All DNS of the tandem cylinder configuration so far revealed the maximum heat transfer to occur downstream of the stagnation point.

The present study investigates the sensitivity of the heat transfer to the wake generator distance. Therefore, an additional embedded DNS is performed with the same Reynolds number as in [5], but with an increased wake generator distance. Since turbulence intensity and wake-deficit of the streamwise velocity decay with increasing wake generator distance, a shift towards the lower regime of [2] is expected. The results will be compared with the data of [5] and the correlations of [1,2]. Of particular interest is the location of maximum heat transfer increase. Finally, flow structures are visualized to see whether the same physical mechanisms as found in [4] are responsible for the heat transfer increase here as well.

CORRELATIONS

In the literature, a number of correlations are available that describe the heat transfer in a stagnation flow. The present simulation results will be compared with two correlations describing specifically the heat transfer in cylinder stagnation flow. The first correlation is due to [1], which describes the heat transfer expressed by the Frössling number $Nu/\sqrt{Re}$ along a cylinder surface by

$$\frac{Nu}{\sqrt{Re}} = 0.9449 - 0.51\left(\frac{\theta}{2}\right)^2 - 0.596\left(\frac{\theta}{2}\right)^4 + \dots \quad (1)$$

where θ is the angle with respect to the stagnation point in radians and Re the Reynolds number ($= U_\infty D/\nu$). This correlation is valid for laminar flow only, for $\theta < 55^\circ$. The Nusselt number, Nu, is defined as

$$Nu = \frac{T_0}{T_0 - T_w} \left.\frac{d(T/T_0)}{d(r/D)}\right|_{wall} \quad (2)$$

with r being the wall-normal coordinate, D the diameter of the cylinder, T_0 the free-stream temperature and T_w the wall temperature. From this correlation it can be observed that the maximum heat transfer occurs at the stagnation point ($\theta = 0^\circ$). Therefore the stagnation point heat transfer is the focus of many other studies. However, for turbulent flow with oncoming wakes, the results of [4, 5] show a shift of the maximum heat transfer off the stagnation line.

In [2] the stagnation point heat transfer was investigated for cylinders and airfoils under the influence of free-stream turbulence and the following correlation from a survey of experimental data was found:

$$\begin{aligned} &Nu_a Pr^{-0.37} = \\ &0.571 + 0.0125\, Tu_a \left\{1 + \tfrac{1.8}{[1+(Tu_a/20)^3]}\right\} \end{aligned} \quad (3)$$

with the characteristic Nusselt number $Nu_a = Nu/\sqrt{a_1 Re}$, the characteristic turbulence intensity $Tu_a = Tu\sqrt{Re/a_1}$, where a_1 is the free-stream strain rate, and the Prandtl number $Pr = 0.7$. The turbulence intensity is defined as $Tu = \sqrt{\frac{2K}{3}}/U_\infty$ with $K = \frac{1}{2}(\langle u'u'\rangle + \langle v'v'\rangle + \langle w'w'\rangle)$, where $\langle\cdot\rangle$ represents the time-average of a quantity. The correlation (3) plotted in figure 7 below indicates the existence of two regimes for the dependency of the heat transfer on the characteristic turbulence level. With help of a simple binomial series, it can be shown that for $Tu_a < 20$ the correlation (3) simplifies to:

$$Nu_a Pr^{-0.37} \approx 0.571 + 0.02375\, Tu_a \quad (4)$$

For $Tu_a >> 20$ equation (3) can be reduced to:

$$Nu_a Pr^{-0.37} \approx 0.571 + 0.0125\, Tu_a \tag{5}$$

From equations (4) and (5) it can be observed that for $Tu_a < 20$, the heat transfer depends much stronger on the characteristic turbulence intensity than for large Tu_a values. Furthermore, the two regimes are more or less linear. In the region between the regimes, $Tu_a = O(20)$, the simplifications (4) and (5) are not valid.

As discussed above, an important parameter determining in which regime the resulting data lies is the coefficient a_1, the free-stream strain rate. By definition, a_1 is the acceleration of the near-wall flow around the cylinder. For the stagnation point this means that a_1 is the acceleration of the tangential velocity $\left(\frac{\partial\langle v\rangle}{\partial y}\right)$ of the free-stream. Because of continuity, a_1 is thus equal to the deceleration of mean u-velocity: $-\frac{\partial\langle u\rangle}{\partial x}$ along the symmetry axis $y/D = 0$. This illustrates the importance of the oncoming flow profile, especially the maximum centerline velocity, since this is the velocity that has to be decelerated to zero in the stagnation point. By increasing the wake generator distance, l/D, the wake deficit of the streamwise velocity decreases, leading to an increase of a_1 and, consequently, to a reduction of Tu_a at the stagnation point. Moreover, also the turbulence intensity Tu decays with increasing distance, yielding a further reduction of Tu_a. This double impact of the wake generator distance on Tu_a makes l/D an interesting parameter to be varied.

METHODOLOGY

Computational setup

The baseline numerical setup resembles the experiment in [3] as closely as possible. In figure 1 an overview is given. The length of the domain is chosen as $15D$. A large heated cylinder with diameter D represents in its front part the leading edge of a turbine blade, the axis of the large cylinder is located at $7.5D$ from the inflow plane. To reduce the vortex shedding behind the large cylinder, a splitter plate with a length of $1.5D$ is placed at the rear. The wake generator is a smaller cylinder with a diameter of $0.25D$, placed upstream of the large cylinder. A baseline wake generator distance l of $2D$ is chosen in accordance with [3]. The channel has a height of $5.2D$ and a width of $2.5D$ and thereby represents the full wind tunnel of the experiments. The blockage of the large cylinder relative to the tunnel cross-section is 19.2%, which is relatively severe. For the second simulation the wake generator distance is increased to $l/D = 3$. Simultaneously, the domain length is increased $1D$ upstream, to a total length of $16D$. The cylinder surfaces and the splitter plate are modeled as no-slip walls. Since the boundary layer thicknesses on the wind tunnel walls are unknown, all tunnel walls are modeled as frictionless walls. The temperature can be calculated by a scalar transport equation, since the flow is incompressible. On the large (heated) cylinder a Dirichlet boundary condition is applied with a temperature of $1.35T_0$. The inflow is uniform and the Reynolds number based on D and the bulk velocity is $48,000$. No freestream turbulence is applied, since this did not have a significant influence in the experiments. For this Reynolds number the wake characteristics of the wake generator were determined in [3]. The heat transfer measurements were performed at even higher Reynolds numbers ($67,500 - 112,000$), which are beyond the reach of the present study. Therefore, only a qualitative comparison of the heat transfer with the experiments is possible.

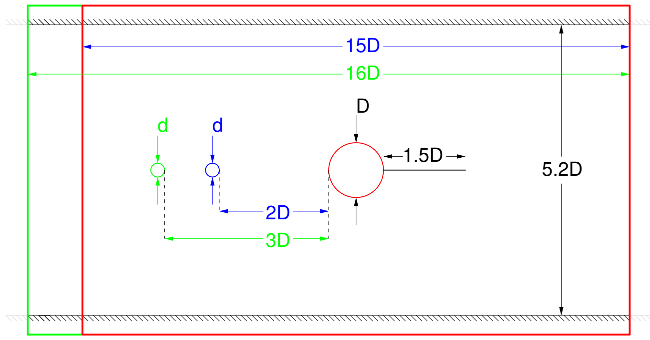

FIGURE 1: Schematic overview of the computational setup with the two wake generator distances.

Numerical method

The simulations were performed with the Finite Volume code LESOCC2 [6, 7] developed at KIT and tested in many previous DNS and LES calculations (e.g. [8, 9]). LESOCC2 solves the incompressible, three-dimensional, time-dependent, Navier–Stokes equations and an arbitrary number of scalar transport equations using second-order accurate central differences for the discretization of the convective and viscous fluxes (and a second-order upwind scheme for the convective terms in the scalar transport). Time advancement is accomplished by an explicit, third order low-storage Runge–Kutta method. An adaptive timestep is chosen, whereby a CFL number of 0.5 is guaranteed. Conservation of mass is achieved by the SIMPLE algorithm with the pressure–correction equation being solved with the strongly implicit procedure (SIP) of Stone. Velocity and pressure decoupling is avoided by a momentum interpolation technique. In the LES zone, the subgrid-scale model of Smagorinsky is used with $C_s = 0.1$. Parallelization is achieved via domain decomposition with the use of ghost cells and MPI for the data transfer. The baseline case is averaged over a timespan of $50D/U_\infty$, for the $l/D = 3$ case this is $55D/U_\infty$. Additionally, both simulation results are averaged in the spanwise direction. The current simulations of $l/D = 2$ and $l/D = 3$ are performed on a Linux cluster, with 256, respectively 276, processors. For the $l/D = 2$ case, a total of 150,000 CPU hours was used, the $l/D = 3$ case took 165,000 CPU hours.

Grid

The computational domain is meshed with a block-structured grid, with a total number of 100 millions cells for the baseline case and 115 million cells for the $l/D = 3$ case. The grid of the $l/D = 3$ case originates from the $l/D = 2$ case, which is shown in figure 2. At $x = -1.5$, where the mesh is relatively uniform in x and y-direction, a cut is made and additional blocks are added. In this way the main elements, the wake generator grid and stagnation region grid, remain intact. The region of interest, the front part of the large cylinder, has the highest cell density. The front half of the large cylinder is meshed with 400 cells in azimuthal direction, the rear half with 240. The smaller wake generator is uniformly meshed with 480 cells in the azimuthal direction. In the spanwise direction 250 cells are used, equidistantly spread along the full channel width. Preliminary studies were performed with lower resolutions and/or a smaller domain width. In table 1 an indication of the achieved resolution is given in terms of nondimensional wall units. The resolution is not as good as one would like, but the results presented below show that it is sufficient for the conclusions drawn. The wake generator is resolved *"just well enough,"* such that the large coherent structures, which will reach the heated cylinder, are well resolved. The smaller structures, which would be dissipated before reaching the stagnation point, are of less importance. Due to the high Reynolds number, a full DNS would be too costly, therefore, a coupling with LES is realized for $x/D > 0$ to save further grid points and hence computational cost.

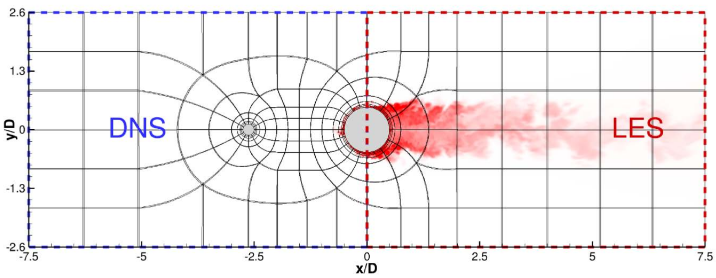

FIGURE 2: Block boundaries. Each block has 40x40 cells in the xy-plane. Indicated are the DNS zone ($x/D < 0$) and the LES zone ($X/D > 0$). The contour gives an impression of the temperature field in the wake of the heated cylinder.

Case	Δr^+	$\Delta\theta^+$	Δz^+
$l/D = 2$	1.32	27.5	34.2
$l/D = 3$	1.42	29.6	36.8

TABLE 1: Maximum grid-spacings in wall-units for $l/D = 2$ and $l/D = 3$, in the region of interest ($-30^\circ \leq \theta \leq 30^\circ$).

RESULTS

As discussed above, the increase of the wake generator distance l/D causes a change of the flow characteristics relevant for the heat transfer increase. Before discussing this effect, first the changes of the flow field characteristics of the oncoming wake are presented.

Flow field comparison

This section focuses on the relevant flow parameters used in correlation (3) for the stagnation point heat transfer. These parameters are: Re, $\langle u \rangle$ and Tu. Since the Reynolds number is kept constant, it is left out of the discussion here. The time-averaged u-velocity and turbulence intensity were also determined in the experiments in [3], where a centerline velocity of $0.721U_\infty$ and a turbulence intensity $Tu = 21\%$ are reported at the location of the stagnation point, but with the large cylinder absent. As already shown in [5], the large cylinder is known to have a considerable influence on the development of the wake, making it questionable whether these values are representative for the actual oncoming flow. For the present simulations the flow characteristics are determined in situ.

In figure 3 the wake profiles of the mean u-velocity are plotted for both simulations. Close to the wake generator, the flow fields of both simulations are almost identical, as illustrated in figure 3a. Close to the heated cylinder stagnation point, however, the wake deficit of the mean velocity for $l/D = 3$ is smaller than for the smaller wake generator distance. This is better shown in figure 4, here the mean streamwise velocity and turbulence intensity are plotted. Figures 4a and 4b show the same data set, however, with a horizontal shift of the coordinate system. From figure 4a the wake development just downstream of the wake generator can be compared. As seen already, the wake in the near vicinity of the wake generator ($-2.5 \leq x/D \leq -2.0$) is nearly identical for both cases, however for $x/D > -2.0$ deviations can be observed. Since all other flow and boundary conditions are identical for both cases, it can be concluded that the influence of the large cylinder reaches at least $1.5D$ upstream, which is almost the complete wake generator distance in case of the smaller spacing $l/D = 2$. Concentrating on the mean velocity, the maximum velocity in the $l/D = 3$ case is markedly higher and further downstream than for $l/D = 2$. To determine the consequences of this increase and shift of the maximum velocity on the stag-

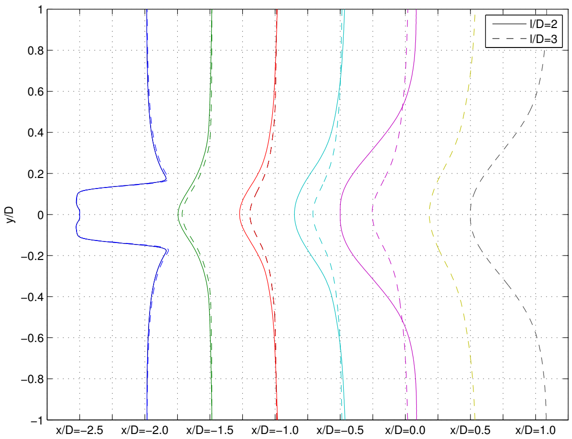

(a) Wake generators coincide

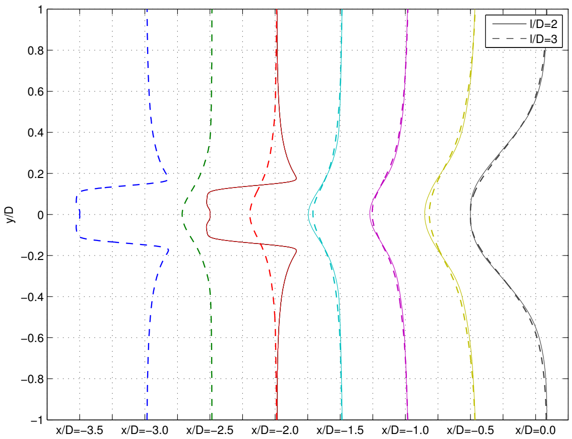

(b) Stagnation points coincide

FIGURE 3: Wake profiles of the mean u-velocity between the wake generator and the heated cylinder stagnation point. The labels are placed where $\langle u\rangle/U_\infty = 1$. In (a) the coordinates of the wake generator coincide; in (b) the x-coordinate is shifted such that the stagnation points coincide.

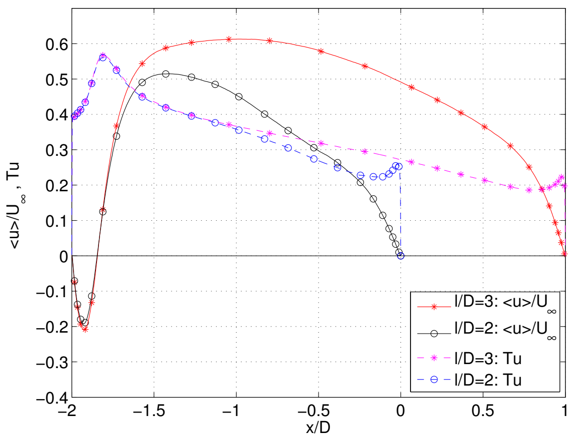

(a) Wake generators coincide

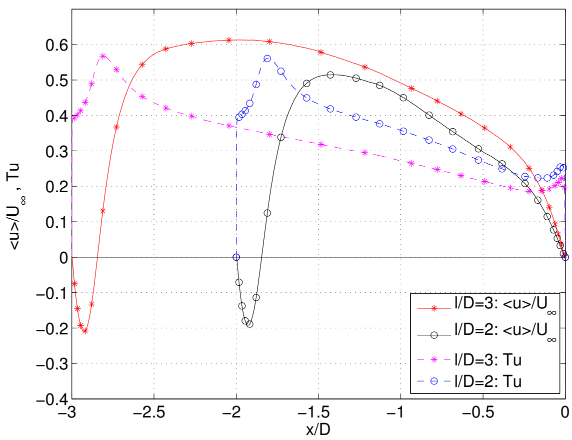

(b) Stagnation points coincide

FIGURE 4: Flow characteristics along the centerline for both wake generator distances l/D. Displayed are the time-averaged streamwise velocity $\langle u\rangle/U_\infty$ and the turbulence intensity Tu; (a) the coordinates of the wake generator coincide; (b) the x-coordinate is shifted such that the stagnation points coincide.

nation region flow characteristics, the coordinates are translated such that the stagnation points of both cases coincide. The result is displayed in figure 4b. As expected, the deceleration at the stagnation point of $\langle u\rangle$ along the centerline is clearly higher for the larger wake generator distance, indicating a larger a_1. Also the turbulence intensity is considerably reduced due to the longer wake development. For $l/D = 2$ a turbulence intensity of 22.5% is found, in the $l/D = 3$ case a turbulence intensity of 18.6% is observed. The value for $l/D = 2$ is actually relatively close to the value found in the experiments of [3] for the same Reynolds number, at the location of the large cylinder but in the absence of it. This indicates that the turbulence intensity is hardly influenced by the large cylinder. This is also observed in figure 4a, the curves for the turbulence intensity show a very similar behavior, though it must be noted that the decay of Tu is slightly slower for the large wake generator distance.

The free-stream strain-rate a_1 was determined to be 1.18 for $l/D = 2$, for $l/D = 3$ a higher value of 1.67 was found, which is to be expected from the previous results. The resulting characteristic turbulence intensity values are $Tu_a = 45.3$ for $l/D = 2$ and $Tu_a = 31.5$ for $l/D = 3$. The higher value is well in the second regime of the correlation (3). The lower value could be regarded as being in the transition region between both regimes.

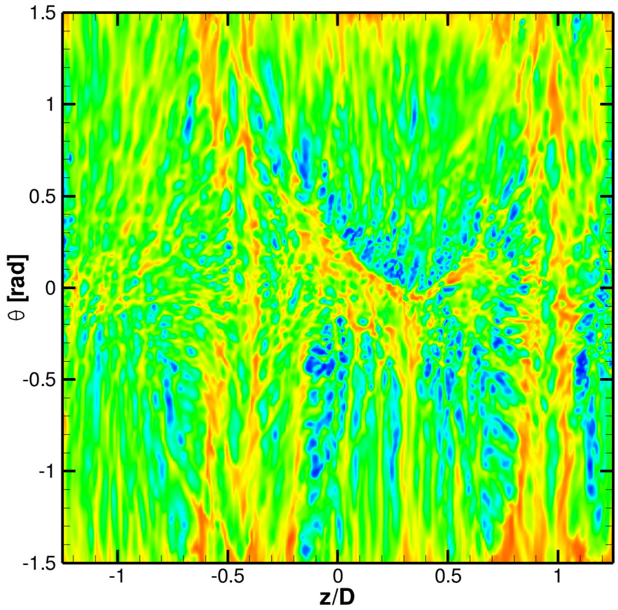

(a) $l/D = 2$

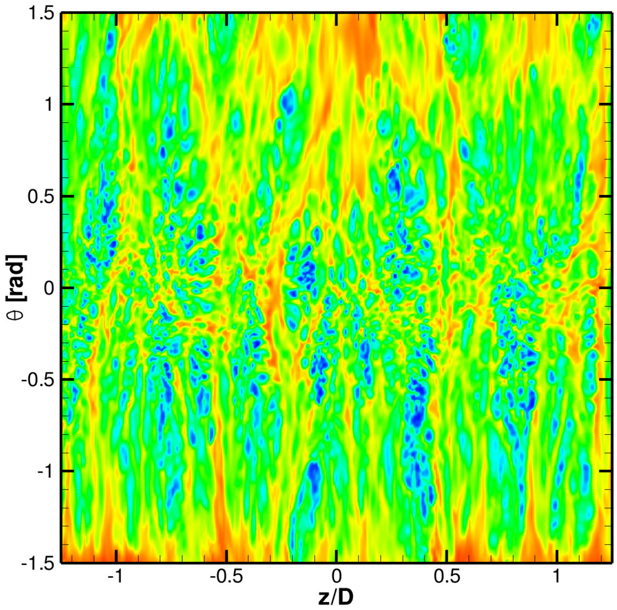

(b) $l/D = 3$

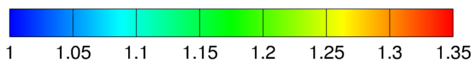

(c) T/T_∞

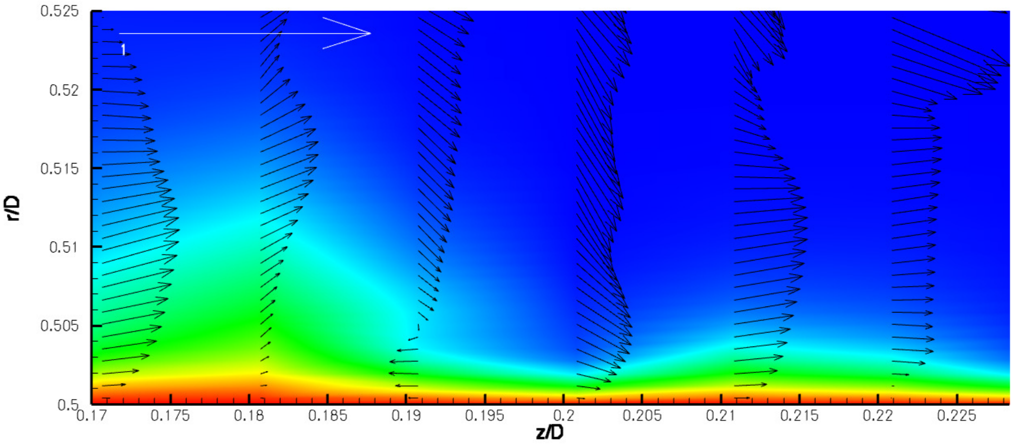

(d) Cut plane normal to the cylinder surface, taken at $\theta = 0$, for $l/D = 3$

FIGURE 5: Instantaneous temperature field adjacent to cylinder surface at $r/D = 0.502$ for both simulations. High cylinder temperature is colored red (dark), low free-stream temperature T_∞ is blue (light).

Instantaneous temperature field

To get a qualitative impression of the heat transfer, in figure 5 the instantaneous temperature field near the heated cylinder is plotted for an arbitrary instant in time for both simulations. The figure shows a curved slice along the front part adjacent to the heated cylinder, which is projected on a 2D plane. The stagnation point is located at $\theta = 0$. Despite the changes in the oncoming flow, the increased wake generator distance does not cause a significant change in the instantaneous temperature field. Both figure 5a and 5b show a similar picture; the fine structured hot and cold spots indicate a turbulent temperature field. In both wake generator distance cases longitudinal structures can be recognized, which is in accordance with the observations in [4]. In [4] these structures are correlated with elongated flow structures around the cylinder that penetrate the boundary layer and influence the heat transfer. As mentioned above, the investigations of [4] cover the lower regime of Tu_a, whereas the present investigations are in the second regime and the transition region in between. The similarity of the heat transfer mechanisms in both regimes is surprising, since the existence of two regimes in a correlation is often related to a change of the responsible mechanism. The present results deny such a conjecture. Finally, in figure 5d a cut-out of the plane normal to the cylinder surface is taken at an arbitrary z-range at the stagnation line. This vector plot demonstrates how heat is transferred due to the turbulent flow and helps understanding the creation of the hot and cold spots on the cylinder surface. At the cold regions there is a strong impingement of the flow and heat is transported sideways, causing hot spots to appear. This effect is strengthened when two side-way flows collide and the heat is trapped.

Comparison with correlations

In the following, a quantitative comparison of the present data with the above described correlations and experiments of [3] is made. The mean heat transfer along the cylinder circumference is displayed in figure 6. As expected, for both simulations the heat transfer has increased with respect to the laminar flow around a cylinder as given in (1). For the small wake generator distance, the effect of the wake deficit of the streamwise velocity is visible, as already shown in [5]. The maximum heat transfer is located at $\theta \approx 30°$, clearly off the stagnation line. This effect is less pronounced for $l/D = 3$, which can be explained by the reduced wake deficit. The experimentally obtained data from [3] also shows a less severe shift of the maximum heat transfer increase. This is consistent, since the heat transfer measurements in the experiments were performed for the lower distance between cylinders but at a higher Reynolds number. The higher Re is expected to also lead to a reduction in the wake deficit.

In figure 7, the correlation from [2] is plotted for the relevant Tu_a range. Recognizable are the two regimes and the transition between them. The gray area represents the bandwidth

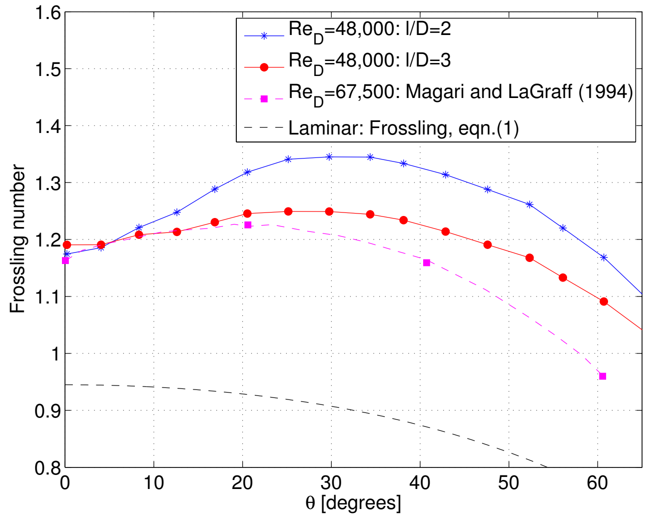

FIGURE 6: Comparison of the numerical simulations with the solution of [1] and experiments of [3], $\theta = 0$ represents the stagnation point.

of the experimental data taken to determine the correlation of equation (3). Note that the data obtained from cylinder data determines the lower bound, whereas the upper bound corresponds to airfoil experiments. The DNS data of the present study show a very good agreement with the correlation. Both for the large and small wake generator distance, the calculated characteristic Nusselt number is on the correlation curve or well within the bandwidth of the experimental data. Also, both data points are located far away from the first linear regime. The good fit with the correlation in the higher Tu_a regime is a promising result, meaning that the higher Reynolds number and Tu_a regimes of the correlation are becoming accessible to DNS studies.

CONCLUSIONS

In the present study, a tandem cylinder setup was simulated by means of embedded DNS. The DNS data show good agreement with the correlation proposed in [2] for all simulations. This correlation exhibits two distinct regimes for the dependency of the heat transfer on a characteristic turbulence level normalized by Reynolds number and the free-stream strain-rate as a measure for the flow acceleration in the free-stream. The data presented here are the only DNS data that reached the regime governed by higher characteristic turbulence levels.

The setup was inspired by experiments performed in [3], in which an increase in heat transfer on the rear cylinder was found due to wake-induced turbulence. Our previous DNS study [5] was able to reproduce this increase in heat transfer for the same setup, but for a lower Reynolds number and with a pronounced

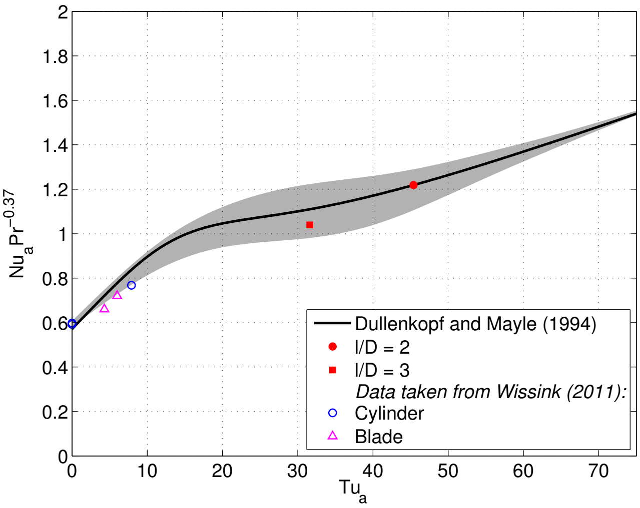

FIGURE 7: Comparison of numerical simulations with the correlation of [2]. The symbols represent numerical simulations from the literature (open symbols) and the present study (filled symbols).

shift of the maximum increase off the stagnation line. For the experiments, such a shift was small for the lowest Reynolds number and completely vanished for higher *Re*. An increase in *Re* was not affordable in our DNS study. Therefore, to investigate the influence of changing wake characteristics without increasing the Reynolds number, the distance between the two cylinders was increased by 50%. The larger wake generator distance allowed for a stronger decay of streamwise velocity wake-deficit and turbulence intensity. This caused a reduction in the characteristic turbulence intensity used for the correlation given in [2] with a value in between the two limiting regimes of the correlation.

The off-stagnation line shift of the maximum heat transfer, as observed for the original cylinder spacing, is only marginally present for the wider spacing which is likely to be due to the reduced wake deficit. Such a reduction is also expected to happen for increased Reynolds numbers, for which the heat transfer measurements were conducted in the experiments. Therefore, our results with larger cylinder spacing are consistent with the experimental observations.

The instantaneous temperature fields reveal no indication of a change in the physical mechanism responsible for the heat transfer increase for all cases investigated. An observation of the instantaneous flow field indicates that elongated flow structures, which penetrate the boundary layer, are responsible for the increase. This is the same mechanism as proposed in [4] for the lower characteristic turbulence levels regime of the correlation.

Overall, it was demonstrated that all regimes of the correlation in [2] are now accessible to (embedded) DNS studies. Moreover, it is possible that somewhat downstream of the stagnation point a larger heat transfer increase has to be expected than is predicted by stagnation point correlations for strong wake deficits reaching a cylinder or airfoil!

ACKNOWLEDGMENT

The work reported here was carried out within the "Research Group Turbo-DNS" at the Institut für Thermische Strömungsmaschinen. Its financial support by the German Excellence Initiative and Rolls–Royce Deutschland is gratefully acknowledged. The authors are grateful for the provision of computer time by the High Performance Computing Center Stuttgart (HLRS) and the Steinbuch Centre for Computing (SCC).

REFERENCES

[1] Frössling, N., 1958. "Evaporation heat transfer and velocity distribution in two-dimensional and rotationally-symmetric laminar boundary layer flow". *NACA TM-1432*.

[2] Dullenkopf, K., and Mayle, R., 1994. "The effects of incident turbulence and moving wakes on laminar heat transfer in gas turbines". *Journal of Turbomachinery,* ***116***, pp. 23–28.

[3] Magari, P., and LaGraff, J., 1994. "Wake-induced unsteady stagnation-region heat transfer measurements". *Journal of Turbomachinery,* ***116***, Jan., pp. 29–38.

[4] Wissink, J., and Rodi, W., 2011. "Direct numerical simulation of heat transfer from the stagnation region of a heated cylinder affected by an impinging wake". *Journal of Fluid Mechanics,* ***doi:10.1017/S0022112010004866***.

[5] Venema, L., von Terzi, D., Bauer, H.-J., and Rodi, W., 2010. "DNS of heat transfer increase in a cylinder stagnation region due to wake-induced turbulence". In Proceedings of 8th International Symposium on Engineering Turbulence Modelling and Measurements - ETMM8 (*Submitted to International Journal of Heat and Fluid Flow by invitation.*).

[6] Hinterberger, C., 2004. "Dreidimensionale und tiefengemittelte Large-Eddy Simulation von Flachwasserströmungen". PhD thesis, University of Karlsruhe.

[7] Breuer, M., and Rodi, W., 1996. "Large eddy simulation of complex turbulent flows of practical interest". In Flow simulation with high performance computers II, volume 52 of Notes on Numerical Fluid Mechanics., E. H. Hirschel, ed., pp. 258–274.

[8] Wissink, J., and Rodi, W., 2008. "Numerical study of the near wake of a circular cylinder". *International Journal of Heat and Fluid Flow,* ***29***(4), pp. 1060–1070.

[9] Garcia-Villalba, M., Li, N., Rodi, W., and Leschziner, M. A., 2009. "Large-eddy simulation of separated flow over a three-dimensional axisymmetric hill". *Journal of Fluid Mechanics,* ***627***, pp. 55–96.